

# DeceptionX: Explainable Deception Detection with Multimodal Large Language Models

Jiayu Zhang\*  
Great Bay University  
Dongguan, Guangdong, China

Yawen Cui  
Hong Kong Polytechnic University  
HongKong, China

Zheng Wang  
Great Bay University  
Dongguan, Guangdong, China

Shuo Ye\*  
Great Bay University  
Dongguan, Guangdong, China

Taorui Wang  
Great Bay University  
Dongguan, Guangdong, China

Haowen Tang  
Great Bay University  
Dongguan, Guangdong, China

Zitong Yu<sup>†</sup>  
Great Bay University  
Dongguan, Guangdong, China

Jiajian Huang  
Great Bay University  
Dongguan, Guangdong, China

Wei Xia  
Great Bay University  
Dongguan, Guangdong, China

Hui Ma  
Great Bay University  
Dongguan, Guangdong, China

## Abstract

Deception detection is a critical and highly challenging task within affective computing and behavioral analysis. Existing deep learning methods typically treat this task as a straightforward classification problem. However, traditional deep binary (truthful/deceptive) models lack interpretability and fails to capture the complex logical deduction processes utilized by human experts when identifying lies. While Multimodal Large Language Models (MLLMs) have shown potential, applying them effectively requires a bridge between mid-level audiovisual cues and high-level logical reasoning. In this paper, we propose DeceptionX, a novel MLLM framework that shifts the paradigm of deception detection from black-box classification to an interpretable Observe-Think-Summarize reasoning process. To address the scarcity of high-quality reasoning data, we first constructed DeceptChain, a high-quality dataset developed through a human-in-the-loop process. This dataset synthesizes fine-grained visual and auditory evidence (such as micro-expressions and vocal tremors) into structured chain-of-thought reasoning data. Furthermore, we propose a three-stage training pipeline and a Discrepancy-Aware Redundancy Elimination (DARE) strategy for DeceptionX to further enhance the model's generalization capabilities. Extensive experiments demonstrate that DeceptionX not only outperforms existing MLLM baselines and state-of-the-art methods on standard real-world benchmarks but also provides transparent, expert-level reasoning paths, bridging the critical gap between accuracy and interpretability in multimodal deception detection.

Permission to make digital or hard copies of all or part of this work for personal or classroom use is granted without fee provided that copies are not made or distributed for profit or commercial advantage and that copies bear this notice and the full citation on the first page. Copyrights for components of this work owned by others than the author(s) must be honored. Abstracting with credit is permitted. To copy otherwise, or republish, to post on servers or to redistribute to lists, requires prior specific permission and/or a fee. Request permissions from [permissions@acm.org](mailto:permissions@acm.org).  
Conference acronym 'XX, Woodstock, NY

© 2018 Copyright held by the owner/author(s). Publication rights licensed to ACM.  
ACM ISBN 978-1-4503-XXXX-X/2018/06  
<https://doi.org/XXXXXXXX.XXXXXXX>

## CCS Concepts

• Computing methodologies → Artificial intelligence.

## Keywords

Deception detection, multimodal understanding

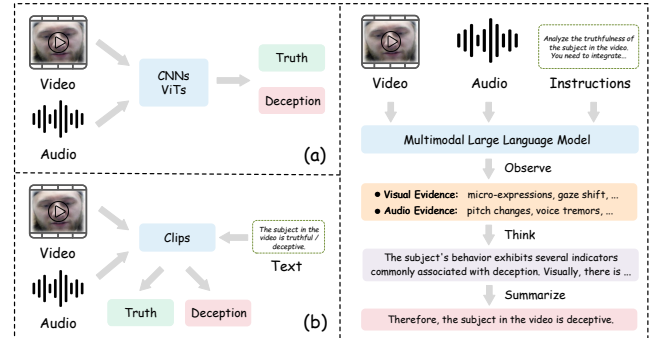


**Figure 1: Compared to traditional feature-based (a) and alignment-based (b) paradigms, DeceptionX shifts from black-box binary classification to an explainable framework that mimics human cognition. By integrating multimodal cues including micro-expressions and voice tremors, DeceptionX follows an Observe-Think-Summarize pipeline to derive reasoned and transparent deception analysis.**

## 1 Introduction

Deception [27] refers to the act of intentionally misleading others. It is a common and complex human behavior that can pose significant threats to national, political, judicial, and economic security. For instance, in the context of public safety, criminals may conceal their intentions to evade detection, thereby endangering social security. Within the judicial system, the falsification of evidence or the provision of false statements can distort case outcomes, leading

to wrongful convictions or acquittals, undermining legal authority, and eroding public trust. Therefore, the detection and prevention of deception are crucial for maintaining social stability and economic order. Because human judgment is often susceptible to cognitive biases, researchers are dedicated to developing multimodal automated deception detection systems. These systems identify deceptive behaviors by analyzing visual and auditory cues [35, 38, 43–45], including facial micro-expressions and vocal patterns.

Despite significant advancements in existing deep learning-based deception detection methods [19, 39, 42], they typically treat the task as a straightforward black-box binary classification problem, as illustrated in Figure 1. This paradigm suffers from two distinct limitations. First, black-box models lack interpretability, failing to capture the complex logical reasoning processes that human experts rely on when identifying lies. In high-stakes real-world applications, a standalone predictive label is far from sufficient; investigators require a verifiable chain of evidence that links low-level audiovisual cues (e.g., gaze shifts, variations in vocal tone) to the final decision. Second, high-level visual cognitive tasks face the challenge of weak semantic correlation between discrete labels and visual content. Traditional classification labels struggle to encompass the subtle, dynamic nuances inherent in deceptive behavior.

In recent years, Multimodal Large Language Models (MLLMs) have demonstrated significant potential for semantic understanding and reasoning [2, 41]. However, existing MLLMs primarily focus on enhancing general capabilities such as video question answering, video captioning, object segmentation, and video content understanding. Their ability to discern deceptive behavior in videos remains limited. Consequently, effectively applying these models to the field of deception detection faces two major challenges. First, there is a lack of comprehensive and structured instructional data capable of clearly identifying, analyzing, and integrating potential deceptive behaviors within videos. Simply prompting off-the-shelf MLLMs often results in superficial judgments devoid of solid evidential grounding. Second, appropriate training strategies to distinctly enhance the model’s analytical and deductive reasoning capabilities in this highly specialized domain have yet to be fully explored.

To address these challenges, we propose an automated construction method and introduce a new dataset named DeceptChain. To reduce the difficulty of annotation, we primarily rely on large language model generation with human assistance to create an automated annotation pipeline. The entire process is conducted in stages where we first extract detectable evidence of suspicious behavior from both visual and auditory perspectives, then further investigate the underlying deceptive processes based on this evidence, and finally merge all annotated attributes to form a coherent chain of reasoning. To bridge the gap between judgment accuracy and interpretable reasoning, we also propose a multimodal deception detection model named DeceptionX based on DeceptChain along with a progressive training strategy. Specifically, we first align audiovisual evidence with multimodal features within the text space, then employ instruction tuning to teach the model basic reasoning regarding the subjects’ behavior in videos and response formatting, and finally utilize reinforcement learning to enhance its accuracy and reasoning rationality in deception detection. Furthermore, we introduce a Discrepancy-Aware Redundancy Elimination (DARE)

strategy to enhance the model’s attention toward suspicious deceptive segments. In summary, our main contributions include:

- We construct DeceptChain, the first high-quality deception detection dataset developed through a comprehensive human-in-the-loop process, which addresses the scarcity of reasoning data in deception detection by synthesizing fine-grained visual and auditory evidence into structured and logical chain-of-thought formats.
- We propose DeceptionX, a novel MLLM framework that shifts the deception detection paradigm from uninterpretable black-box classification to a transparent, human-like Observe-Think-Summarize reasoning process.
- We design a progressive three-stage training pipeline and introduce a Discrepancy-Aware Redundancy Elimination (DARE) strategy to significantly enhance the model’s analytical focus and generalization capabilities.
- Extensive experiments demonstrate that DeceptionX outperforms existing MLLM baselines and state-of-the-art methods across multiple benchmarks and cross-domain tests, while providing transparent, expert-level reasoning paths.

## 2 Related Works

### 2.1 Automated Deception Detection

Automated deception detection [10, 12] represents a formidable and essential task within the fields of affective computing and behavioral analysis. The developmental trajectory of this field has transitioned from traditional feature engineering [6, 11, 16] to sophisticated deep learning architectures. While early research relied heavily on psychological priors and manually crafted statistical features, the widespread adoption of deep neural networks [1, 3, 13, 20, 22, 28] has significantly improved detection accuracy by processing data in an end-to-end fashion. Despite these performance gains, prevailing deep learning methods typically treat deception detection as an opaque binary classification problem. In high-stakes real-world scenarios such as judicial proceedings and security screenings, providing an isolated predictive label is insufficient. Systems must instead offer a verifiable chain of evidence that connects fundamental audiovisual cues including micro-expression variations, vocal tremors, and gaze shifts to the final decision-making process. In this paper, we leverage MLLM to generate text-based reasoning chains that provide interpretability for the entire process.

### 2.2 Multi-modal Large Language Models

In recent years, Multimodal Large Language Models (MLLMs) [7, 9, 25, 37] have demonstrated exceptional capabilities in cross-modal semantic understanding and high-level reasoning. Unlike traditional deep learning models that are constrained to specific tasks, MLLMs leverage the vast knowledge and linguistic reasoning inherent in large language models (such as Qwen series [5, 17]) to process and interpret diverse inputs, including video, audio, and text. Although they have achieved success in general tasks like video captioning and question answering, applying MLLMs to deception detection still faces several unique challenges. First, existing models often produce false or superficial judgments because they lack fine-grained, domain-specific instruction tuning to identify subtle deceptive cues such as micro-expressions or vocal tremors.

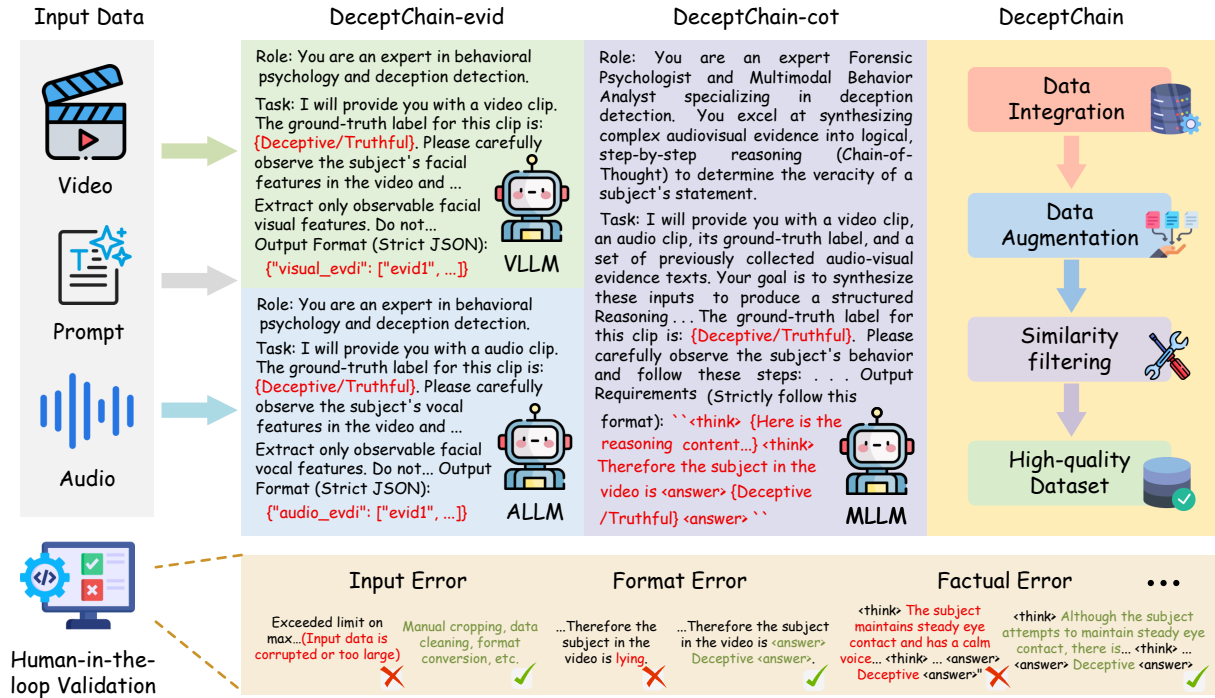


Figure 2: The construction pipeline of our proposed instruction datasets (DeceptChain-evid, DeceptChain-cot, and DeceptChain), follows a model-led and human-assisted annotation strategy designed to ensure high label quality at scale. By leveraging human priors to guide the generation of descriptions and the refinement of samples through a multi-stage pipeline involving LLM-based filtering, keyword heuristics, and manual verification, we achieve the automated annotation of large-scale data.

Table 1: Comparison of different multimodal deception detection datasets. “-” indicates that there is no relevant information.

Dataset	Videos	Deceptive	Truthful	Annotation	Setting	Label	Auto pipeline
Real Life Trials [31]	121	61	60	-	Courtroom	Binary Classification	✗
POLLY [4]	146	73	73	-	Public Speech	Binary Classification	✗
Bag of Lies [15]	325	162	163	-	Laboratory	Binary Classification	✗
MU3D [26]	320	160	160	-	Laboratory	Binary Classification	✗
Box of Lies [33]	1049	862	187	-	Game Show	Binary Classification	✗
DOLos [14]	1675	899	776	-	Game Show	Binary Classification	✗
<b>DeceptChain(Ours)</b>	<b>2230</b>	<b>1221</b>	<b>1009</b>	<b>6690</b>	<b>Cross-scene</b>	<b>Reasoning Analysis</b>	<b>✓</b>

Second, existing frameworks primarily focus on content understanding rather than the complex, expert-level logical deduction required for behavioral analysis.

To bridge this gap, we propose the DeceptionX framework, which enhances these general MLLM capabilities through a multi-stage pipeline. We also introduce a specialized instruction dataset, DeceptChain, which mimics the human cognitive pattern of “Observe-Think-Summarize”. This approach directly links low-level audio-visual evidence to the final veracity judgment, ensuring that the model’s reasoning is both accurate and verifiable.

### 3 DeceptChain

A significant bottleneck in applying Multimodal Large Language Models (MLLMs) to deception detection is the lack of domain-specific datasets that provide fine-grained reasoning. To bridge this gap, we introduce DeceptChain, a high-quality instruction tuning dataset. As shown in Table 1, unlike existing datasets [31, 33] that restrict deception to a binary classification label, DeceptChain is explicitly designed to support detailed reasoning analysis. It was constructed from existing deceptive-scene video data [14, 15, 26] and contains 2,230 videos in total, including 1,221 deceptive samples and 1,009 genuine samples, along with 6,690 rich annotations. To construct this dataset efficiently while ensuring expert-level quality, we design a model-led and human-assisted annotation strategy. As

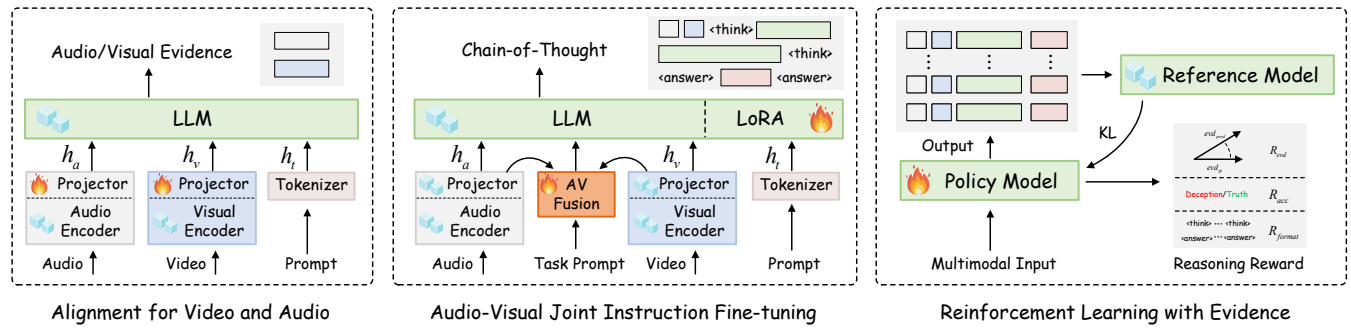


**Figure 3: The three-stage training framework of DeceptionX: (1) Audio-video feature alignment: align multimodal audio and video evidence into the text feature space. (2) Joint audio-video instruction tuning: instruction-tune the model using chain-of-thought data so it acquires fundamental reasoning abilities about the subject’s behavior. (3) Evidence-based reinforcement learning: optimize the policy model with reasoning-based reward mechanisms to further improve deception detection accuracy and the plausibility of its logical inferences.**

illustrated in Figure 2, the data generation pipeline is divided into evidence extraction, chain-of-thought synthesis, and human-in-the-loop validation.

### 3.1 Multimodal Evidence Extraction

Directly prompting an MLLM to analyze a raw video often yields superficial or hallucinated reasoning. Therefore, the first stage of our pipeline isolates the extraction of low-level behavioral cues to create the DeceptChain-evid sub-dataset. We employ specialized Vision Large Language Models (Qwen2.5-VL [37]) and Audio Large Language Models (Qwen2-Audio [8]). We design specific prompts instructing these models to act as experts in behavioral psychology and deception detection. Given the raw video or audio clip alongside its ground-truth label, the VLLM extracts observable facial features (e.g., micro-expressions, gaze shifts), while the ALLM identifies distinct vocal characteristics (e.g., voice tremors, pitch variations). To ensure downstream compatibility, the models are constrained to output these extracted attributes in a strict JSON format.

### 3.2 CoT Reasoning Aggregation

After extracting low-level multimodal cues, the next core challenge is how to synthesize these isolated, fine-grained visual and auditory evidences into a coherent and logically consistent higher-order reasoning chain. To this end, we employ a powerful multimodal large language model at this stage as an expert to build the bridge from low-level audio-visual evidence to high-level logical inference. The inputs to this stage include not only the original video and audio clips and the ground-truth labels, but also the structured, human-vetted collection of audiovisual evidence texts produced in the previous stage. To ensure that the generated reasoning data attains expert-level quality and depth, we configure the MLLM to act as a courtroom psychologist and multimodal behavioral analysis expert specializing in deception detection. The model is explicitly instructed to closely observe the subject’s dynamic behavior and to deeply fuse and deduce from the previously collected audio-visual cues. For example, the model must, based on the provided cues, explain why changes in micro-expressions (such as gaze aversion) together with anomalous voice features (such as pitch shifts or

trembling) jointly point to deceptive intent in a particular context. Finally, to satisfy the strict data-structuring requirements of the subsequent instruction-tuning stage, we impose mandatory constraints on the MLLM’s output format. The data subset generated by this automated and heuristic-combined process, DeceptChain-cot, not only endows the dataset with unprecedented explanatory richness but also provides high-quality structured reasoning supervision signals for DeceptionX.

### 3.3 Human-in-the-loop Validation

Although LLMs perform excellently at text generation, they occasionally produce formatting errors or semantic hallucinations. To ensure high quality for large-scale annotation, we introduced a strict human-in-the-loop verification mechanism. Human annotators and automated heuristic scripts are used to filter out three main types of anomalies. Input errors: samples with corrupted input data or those that exceed maximum processing limits are discarded. Formatting errors: to prevent parsing failures during model training, generated outputs that do not conform to the required `<think>` and label structure are rejected. Factual errors: annotators review the text to ensure that the reasoning aligns perfectly with behaviors observable in the video and the true labels (for example, rejecting samples where the text describes “steady eye contact and a calm voice” but the model reached a misleading conclusion). After the validation stage, the final DeceptChain dataset undergoes dataset integration, data augmentation, and similarity filtering. This postprocessing approach guarantees diversity, nonredundancy, and high quality of the corpus and provides the necessary foundation for training our interpretable DeceptionX framework.

## 4 DeceptionX

Our goal is to enhance the deception detection capability of MLLMs. To this end, we adopt the progressive multimodal training paradigm shown in Figure 3, designed to enable MLLMs to transition from identifying suspicious behavior to reasoning about and summarizing the deception process. In this section, we introduce DeceptionX, a framework specifically designed for deception detection.

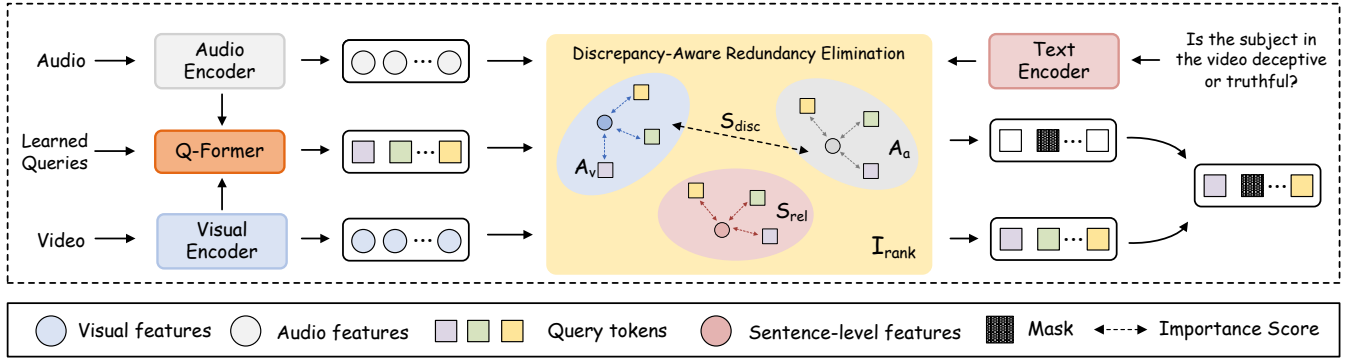


**Figure 4: Architecture of the AV-fusion and Discrepancy-Aware Redundancy Elimination (DARE).** Features are temporally concatenated and fused with learnable queries via a Q-Former to produce compact multimodal representations. DARE then computes sentence-level importance scores to identify suspicious deceptive segments, applies dynamic masking to eliminate redundant or low-salience information (grayed out), and retains only highly relevant cues.

#### 4.1 Pretraining based on audio-visual evidence

In the first stage, our objective is not to have the model produce a binary true/false judgment directly, but to first establish a robust multimodal evidence alignment capability that enables it to recognize and extract verifiable low-level cues from raw video and audio. Specifically, the model receives video frames and their corresponding audio, encodes them, and maps them into a unified textual semantic space. During this process, the model is constrained to attend to observable signals that are highly relevant to deceptive behavior, such as microexpressions, gaze shifts, tonal variations, and vocal tremor, thereby forming preliminary correspondences between audiovisual cues and textual semantics. This stage functions as a perceptual foundation for subsequent reasoning, teaching the model to see the evidence before explaining it, and emphasizes strengthening downstream learnability and interpretability through multimodal evidence alignment. Visual and audio signals are processed separately through their respective encoders and projectors, and can be expressed formally as follows:

$$\begin{aligned} h_a &= \text{Projector}_a(\text{Encoder}_a(f_a)) \\ h_v &= \text{Projector}_v(\text{Encoder}_v(f_v)) \end{aligned} \quad (1)$$

The prompt is converted into  $h_t$  by the tokenizer. To enhance the alignment of Audio/Video-Language modeling, we freeze LLM and the pre-trained encoder, and fine-tune only the projector.

#### 4.2 Chain-of-thought Supervised Fine-Tuning

After completing evidence alignment, the second stage introduces Chain-of-Thought (CoT) data for instruction fine-tuning to transition the model from evidence recognition to causal reasoning. Training samples in this stage include not only the raw audiovisual inputs and ground truth labels but also the structured evidence texts generated in the previous stage and manually verified. The model is required to analyze suspicious behavior and then explain why these cues jointly indicate deceptive intent using a fixed format such as <think> and <answer>. This training regime does not merely increase output length but explicitly teaches the model to follow an expert reasoning chain of observe, think and summarize,

organizing local audiovisual cues into a coherent and verifiable logical process. Additionally, in this stage we introduce an audio-visual fusion module in which temporal information is preserved in the visual features  $h_v$  and the audio features  $h_a$  and Q-Former [21] is used for multimodal fusion. Concretely, to compress the multimodal content, we first create  $K$  learnable query tokens  $h_q \in \mathbb{R}^{Kd}$ . Then, through cross-attention,  $h_q$  interacts with the concatenated  $h_c$  to distill knowledge from the multimodal content into the query tokens. Formally, this process is expressed as:

$$\begin{aligned} h_c &= \text{Concat}(h_a, h_v) \\ h_f &= \text{Q-former}(h_q, h_c + \text{PE}(h_c)) \end{aligned} \quad (2)$$

where  $h_c \in \mathbb{R}^{(t_a+t_v) \times d}$ , with the concatenation operation applied along the temporal dimension. Here,  $h_f \in \mathbb{R}^{K \times d}$ , and  $\text{PE}(\cdot)$  represents the positional encoding.

#### 4.3 Reinforcement Learning with Evidence

Although the preceding stages have endowed DeceptionX with robust multimodal evidence alignment and basic chain-of-thought reasoning capabilities, the model still requires explicit optimization to simultaneously maximize detection accuracy and the logical plausibility of its inferences. To this end, we introduce the third training stage (evidence-based reinforcement learning) that refines the policy model  $\pi_\theta$  (the MLLM after CoT supervised fine-tuning) by directly optimizing a composite reward that evaluates both veracity judgments and their grounding in low-level audiovisual cues. Formally, given a multimodal input  $x = (v, a, t)$  (video frames, audio, and prompt), the policy  $\pi_\theta$  generates structured evidence  $e$  and a reasoning trace <think>  $\dots$  <think>, followed by a final binary label  $y \in \{\text{Deceptive}, \text{Truthful}\}$ . Inspired by GRPO [32], our reward function consists of three components: a format reward ( $\mathcal{R}_{format}$ ), an accuracy reward ( $\mathcal{R}_{acc}$ ) and an evidence reward ( $\mathcal{R}_{evid}$ ).

**Format Reward ( $\mathcal{R}_{format}$ ).** To ensure structured outputs, we define a binary reward function that checks whether the model’s response contains evidence, a reasoning section, and an answer section. It returns 1.0 if all are present and -1.0 otherwise:

$$\mathcal{R}_{\text{format}}(o|v, a, t) = \begin{cases} +1.0, & \text{is\_required\_format}(o) \\ -1.0, & \text{otherwise} \end{cases} \quad (3)$$

**Accuracy Reward ( $\mathcal{R}_{\text{acc}}$ ).** To force the DeceptionX to produce a clear detection category, we strictly constrain the output space. The label reward gives a positive reward for exact matches and penalizes incorrect guesses. In addition, if the model fails to output a categorical conclusion, it receives a severe penalty. The formulation is as follows:

$$\mathcal{R}_{\text{acc}}(o|v, a, t) = \begin{cases} +1.5, & o^a = y^a \\ -1.5, & \text{not } o^a \\ -1.0, & \text{otherwise} \end{cases} \quad (4)$$

**Evidence Reward ( $\mathcal{R}_{\text{evd}}$ ).** To further improve the reasoning accuracy of DeceptionX, we impose constraints on the areas where the model is prone to hallucinations, specifically the audiovisual evidence section. In particular, we define a semantic threshold and reward reasoning samples that exceed this value to establish grounded reasoning behavior. The formulation is as follows:

$$\mathcal{R}_{\text{evd}}(o|v, a, t) = \begin{cases} \text{Cos}(o^{\text{evd}}, y^{\text{evd}}) & \text{greater than threshold} \\ -1.0, & \text{otherwise} \end{cases} \quad (5)$$

where  $\text{Cos}(\cdot)$  computes the semantic similarity between the generated evidence and the ground truth. After undergoing three stages of training according to the progressive strategy described above, the MLLM’s deception detection capability is improved.

#### 4.4 Redundancy Elimination Strategy

Although the Q-Former compresses the temporally concatenated audiovisual features  $h_c$  into a compact set of  $K$  fused tokens  $\{z_i\}_{i=1}^K$ , long-duration deceptive videos inevitably contain substantial redundant or background information that dilutes model attention on sparse, diagnostically critical cues such as micro-expressions and vocal tremors. To dynamically prioritize suspicious segments while eliminating low-salience tokens, we introduce the Discrepancy-Aware Redundancy Elimination (DARE). As illustrated in Figure 4, DARE is seamlessly integrated after the Q-Former within the AV-fusion module and operates directly on the fused representations before they are fed to the LLM. DARE computes a per-token importance score  $I_{\text{rank}}$  by combining two complementary signals specifically tailored to deception detection: prompt-anchored semantic relevance and cross-modal discrepancy mining.

**Prompt-Anchored Semantic Relevance Assessment.** To suppress tokens that capture irrelevant background noise unrelated to the deception/honesty judgment task, we first evaluate the semantic alignment of each fused token  $z_i$  with the task-specific prompt features  $t_s$  (derived from the input instruction). We compute the maximum cosine similarity across all prompt tokens:

$$S_{\text{rel}}^{(i)} = \max_{j \in [1, M]} \left( \frac{z_i \cdot t_s}{\|z_i\| \|t_s\|} \right) \quad (6)$$

this mechanism explicitly anchors token importance to the core semantics of the deception detection pipeline, ensuring that only cues relevant to behavioral analysis are retained.

---

#### Algorithm 1 Discrepancy-Aware Redundancy Elimination (DARE)

---

**Require:** Fused tokens  $\{z_i\}_{i=1}^K$ , prompt features  $t_s$ , visual features  $\{h_n^v\}_{n=1}^{N_v}$ , audio features  $\{h_n^a\}_{n=1}^{N_a}$ , weight  $\omega$

**Ensure:** Masked tokens  $\mathcal{Z}_{\text{sel}}$

- 1: **for** each token  $z_i$  **do**
- 2:   Compute semantic relevance:
- 3:      $S_{\text{rel}}^{(i)} = \max_{j \in [1, M]} \left( \frac{z_i \cdot t_s}{\|z_i\| \|t_s\|} \right)$
- 4:   Compute audio-visual affinity:
- 5:      $D_t = 1 - \cos(h_{v,t}, h_{a,t})$
- 6:   Compute discrepancy score:
- 7:      $S_{\text{disc}}^{(i)} = \sum_{t=1}^T \alpha_{i,t} \cdot D_t$
- 8: **end for**
- 9: Normalize  $\{S_{\text{rel}}^{(i)}\}$  and  $\{S_{\text{disc}}^{(i)}\}$
- 10: **for** each token  $z_i$  **do**
- 11:   Compute importance:
- 12:      $I_i = \omega S_{\text{rel}}^{(i)} + (1 - \omega) S_{\text{disc}}^{(i)}$
- 13: **end for**
- 14: Select  $K$  tokens or those with  $I_i < \tau$
- 15:  $\mathcal{Z}_{\text{sel}} \leftarrow \{z_i \mid I_i \text{ is selected}\}$
- 16: **return**  $\mathcal{Z}_{\text{sel}}$

---

**Cross-Modal Discrepancy Mining.** A defining characteristic of deceptive behavior is the incongruence between visual and auditory modalities. To explicitly capture such diagnostic contradictions, we measure the differential affinity between the original raw visual feature sequences  $\{f_{v,n}\}_{n=1}^{N_v}$  and the raw audio feature sequences  $\{f_{a,n}\}_{n=1}^{N_a}$ . The specific formulation is as follows:

$$D_t = 1 - \cos(h_{v,t}, h_{a,t}) \quad (7)$$

The cross-modal discrepancy score is then defined as:

$$S_{\text{disc}}^{(i)} = \sum_{t=1}^T \alpha_{i,t} \cdot D_t \quad (8)$$

where  $\alpha_{i,t}$  is the attention weight of  $z_i$  assigned to time step  $t$ . The absolute difference quantifies asymmetric modal responses and the second term amplifies directional inconsistency. Higher values of  $S_{\text{disc}}^{(i)}$  indicate that the token has successfully encoded conflicting multimodal signals, which are precisely the subtle cues human experts rely on to detect deception. The final importance score for each token is obtained via a weighted linear combination after Min-Max normalization ( $\tilde{S}$ ) across all tokens:

$$I_i = \omega \cdot \tilde{S}_{\text{rel}}^{(i)} + (1 - \omega) \cdot \tilde{S}_{\text{disc}}^{(i)} \quad (9)$$

The hyperparameter weight  $\omega \in [0, 1]$  balances these two signals. Tokens with importance scores below the threshold will be masked, ensuring that only high-importance representations are forwarded to the LLM.

## 5 Experiments

In this section, we comprehensively evaluate the effectiveness of the proposed DeceptionX framework on widely-used deception detection benchmarks, including DOLOs [14], Bag of Lies (BoL) [15], and MU3D [26]. We report Accuracy (Acc.) and F1 score to evaluate

**Table 2: Comparisons of DeceptionX with recent MLLMs. We evaluate performance across three datasets: DOLOs, Bag-of-Lies (BoL), and MU3D.**

Method/Model	Modalities	Params	DOLOs			BoL			MU3D		
			Acc.	F1	SEA	Acc.	F1	SEA	Acc.	F1	SEA
<i>Closed Model</i>											
Qwen-VL-Max [37]	Video	-	54.32	51.38	43.42	41.78	43.76	45.52	46.28	42.52	50.86
Gemini2.5Pro [36]	Video + Audio	-	60.32	53.64	68.74	50.74	64.15	67.75	48.64	51.23	54.43
Gemini3Pro [36]	Video + Audio	-	62.13	59.35	70.12	53.38	57.64	55.42	51.86	55.43	56.78
<i>Open Source Model</i>											
Qwen2.5-VL [37]	Video	7B	46.74	53.28	42.21	43.68	42.51	23.47	50.56	52.47	44.83
AffectGPT [23]	Video + Audio	7B	64.08	66.52	68.84	55.43	57.21	69.32	54.98	57.64	68.53
VideoLLaMA2 [7]	Video + Audio	7B	54.24	57.68	60.21	45.85	50.27	52.23	50.78	53.64	54.58
PandaGPT [34]	Video + Audio	7B	52.14	53.56	57.78	47.82	50.23	49.86	51.57	54.21	55.43
Qwen2.5-Omni [40]	Video + Audio	7B	51.16	52.58	57.43	44.37	44.25	51.58	53.56	55.71	60.23
<b>DeceptionX (Ours)</b>	<b>Video + Audio</b>	<b>7B</b>	<b>69.78</b>	<b>73.38</b>	<b>80.14</b>	<b>61.23</b>	<b>63.98</b>	<b>78.82</b>	<b>60.64</b>	<b>61.72</b>	<b>78.43</b>

**Table 3: Comparisons of the proposed DeceptionX with recent methods.**

Model	Reason	DOLOs		BoL		MU3D	
		Acc.	F1	ACC	F1	Acc.	F1
MLP [15]	X	57.49	-	49.90	-	-	-
LieNet [19]	X	56.50	69.72	59.78	58.14	53.48	33.62
FacialCueNet [29]	X	60.98	68.65	56.23	63.26	57.64	59.13
DDABG [18]	X	55.47	62.52	56.66	55.17	55.63	51.99
PECL [14]	X	64.75	71.20	59.51	51.06	56.25	45.72
<b>DeceptionX</b>	✓	<b>69.78</b>	<b>73.38</b>	<b>61.23</b>	<b>63.98</b>	<b>60.64</b>	<b>61.72</b>

**Table 4: Cross-Domain Evaluation on DOLOs (D), Bag-of-Lies (B), and MU3D (M). “X&Y→Z” denotes training on X and Y, testing on Z.**

Method	M&B → D		D&M → B		D&B → M		Average	
	Acc.	F1	ACC	F1	Acc.	F1	Acc.	F1
LieNet [19]	54.40	68.23	54.69	50.51	51.08	59.75	53.39	59.50
PECL [14]	54.51	69.55	51.25	66.95	55.38	52.46	53.71	62.99
<b>Ours</b>	<b>58.32</b>	<b>64.57</b>	<b>56.41</b>	<b>68.74</b>	<b>56.13</b>	<b>58.24</b>	<b>56.95</b>	<b>63.85</b>

the model’s detection performance, and to rigorously evaluate the reasoning capability of our model, we also introduce the Semantic Evidence Alignment (SEA) metric. Unlike traditional n-gram based metrics (e.g., BLEU [30], ROUGE [24]), which fail to capture semantic variations in descriptive cues (e.g., “gaze aversion” or “looking away”), SEA leverages a pre-trained sentence encoder to map visual and audio cues into a high-dimensional semantic space. Specifically, we compute the cosine similarity matrix between the generated semantic evidence and the ground truth. We define a successful reasoning as a semantic match exceeding a threshold  $\tau$ , which allows us to calculate the Precision, Recall, and F1-score for evidence grounding. This ensures that our evaluation reflects the model’s actual perceptual understanding rather than mere lexical overlap. More details can be found in the appendix.


## 5.1 Main Result

**Comparison with MLLM Baselines.** Table 2 reports the quantitative comparison of DeceptionX against recent closed-source and open-source MLLMs across the three benchmarks. DeceptionX consistently achieves the highest Accuracy and F1 scores on all datasets. For example, on DOLOs it reaches 69.78% Acc. and 73.38% F1, outperforming the strongest closed-source baseline Gemini-3-Pro and the best open-source model AffectGPT. More importantly, DeceptionX delivers substantially superior Semantic Evidence Alignment (SEA). These gains validate the effectiveness of our DeceptChain dataset, the progressive three-stage training pipeline, and the Discrepancy-Aware Redundancy Elimination (DARE) strategy in enabling high-quality, human-like Observe-Think-Summarize reasoning while maintaining strong classification performance.

**Comparison with Specialized Deception Detection Methods.** Table 3 further compares DeceptionX with recent state-of-the-art specialized deception detection models (e.g., MLP [8], LieNet [11], FacialCueNet [17], DDABG [10], and PECL [7]). All compared baselines treat deception detection as a black-box binary classification task (denoted X under Reason) and therefore cannot provide interpretable reasoning. DeceptionX not only outperforms these methods across every dataset but also supplies transparent, expert-level reasoning paths. Concretely, it achieves 69.78% Acc. / 72.38% F1 on DOLOs (versus the previous best PECL at 64.75% / 71.20%), 61.23% Acc. / 63.98% F1 on BoL, and 60.64% Acc. / 61.72% F1 on MU3D. The ability to simultaneously deliver superior accuracy and verifiable chain-of-thought explanations demonstrates that shifting from opaque classification to an interpretable MLLM paradigm closes the critical gap between performance and practical usability in high-stakes deception detection scenarios.

**Cross-Domain Generalization.** To further assess the generalization capability of DeceptionX across heterogeneous deception scenarios, we conduct cross-domain experiments following the X&Y→Z protocol (training on any two datasets and testing on the remaining one), as reported in Table 4. DeceptionX consistently outperforms the specialized baselines LieNet and PECL in all transfer settings. Concretely, it achieves the highest average accuracy of

**Table 5: Qualitative comparison on a deceptive behavior video clip. Incorrect/correct answer is highlighted in red/green.**

Video Sample	
	
Ground Truth: Deceptive	
<b>Gemini</b>	Visual evidence: “frequent hand gestures”, “shifting gaze and head turns”; audio evidence: “animated speech with varying tone and pauses” <think>The combination of natural, expressive body language and a conversational, slightly hesitant speech <b>pattern points towards the speaker telling a genuine story</b> . There are no strong indicators of deception such as rigid posture, lack of emotion, or an overly polished delivery.</think> <answer> <b>Truthful</b> </answer>
<b>Qwen</b>	Visual evidence: “expressive gestures”, “open palms”, “natural smiles”, “consistent eye contact”; audio evidence: “fluent speech”, “no hesitations” <think> <b>no microexpressions of stress, relaxed demeanor typical of truth-telling in panel show</b> .</think> <answer> <b>Truthful</b> </answer>
<b>DeceptionX (Ours)</b>	Visual evidence: “gaze deviation”, “slight lip compression”, “fidgeting hands”; audio evidence: “hesitation (‘um)”, “pauses”, “slight pitch variation” <think> <b>The speaker uses hesitant phrasing and pauses, indicating cognitive load. Her gaze shifts slightly away from the interviewer, suggesting discomfort or fabrication. She avoids direct personal pronouns, distancing herself from the narrative. These cues align with deceptive behavior.</b> </think> <answer> <b>Deceptive</b> </answer>

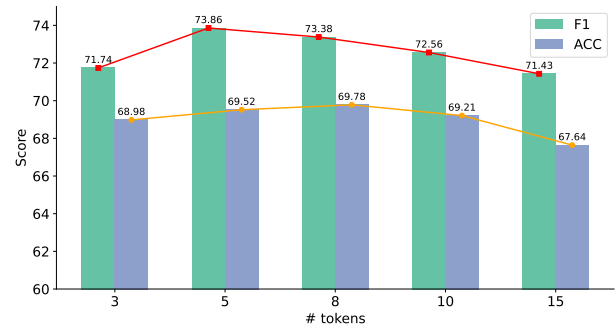
**Table 6: Ablation results across different datasets.**

TPS	DARE	DOLOs		BoL		MU3D	
		Acc.	F1	ACC	F1	Acc.	F1
X	X	64.58	67.02	55.92	57.34	55.42	58.10
X	✓	65.73	68.44	57.32	58.04	56.38	58.12
✓	X	68.53	70.62	60.46	61.83	59.41	60.86
✓	✓	<b>69.78</b>	<b>73.38</b>	<b>61.23</b>	<b>63.98</b>	<b>60.64</b>	<b>61.72</b>

56.95% and F1 score of 63.85%, surpassing the best baseline (PECL) by approximately 3.24% in accuracy and 0.86% in F1. Notably, in the challenging M&B→D transfer, our model reaches 58.32% Acc. and 64.57% F1, while maintaining strong performance in the other two settings (56.41% Acc./68.74% F1 on D&M→B and 56.13% Acc./58.24% F1 on D&B→M). These results demonstrate that our proposed strategies effectively enhance the model’s robustness and practical applicability in real-world, cross-scene deception detection.

## 5.2 Ablation Study

To thoroughly investigate the contribution of each component in the proposed DeceptionX framework, we perform ablation studies on the DOLOs, BoL, and MU3D datasets. As shown in Table 6, we ablate the three-stage progressive strategy (TPS) and the Discrepancy-Aware Redundancy Elimination (DARE) module. The baseline without TPS or DARE yields the lowest performance. Adding DARE alone brings modest but consistent gains by dynamically prioritizing suspicious deceptive segments and suppressing redundant background information. Incorporating the full TPS significantly boosts results across all datasets by progressively establishing multimodal evidence alignment, CoT reasoning, and reinforcement-learning-based optimization. The complete configuration (TPS + DARE) achieves the best performance on every benchmark (69.78% Acc./72.38% F1 on DOLOs, 61.23% Acc./63.98% F1 on BoL, and 60.64% Acc./61.72% F1 on MU3D), confirming that these two components work synergistically to improve both detection accuracy and the quality of interpretable reasoning.

**Figure 5: Ablation study on masked tokens in DARE.**

**Impact of Masked Token Number in DARE.** To further investigate the behavior of the proposed Discrepancy-Aware Redundancy Elimination (DARE), we analyze the effect of varying the number of masked tokens, as illustrated in Figure 5. We vary the number of masked tokens from 3 to 15 and evaluate the performance on DOLOs in terms of Accuracy and F1. The results demonstrate a non-monotonic trend, revealing the trade-off between redundancy removal and information preservation. When the number of masked tokens is small (e.g., 3), the model still retains a large amount of redundant or low-salience information, which distracts the attention from critical deceptive cues and leads to suboptimal performance. As the number of masked tokens increases, the model performance improves and reaches its peak at masking 8 tokens. However, when the number of masked tokens continues to increase, the performance begins to decline. This is because excessive masking removes not only redundant information but also essential discriminative cues. These findings highlight that an appropriate degree of masking is critical for achieving optimal performance.

## 5.3 Visualization and Discussion

Table 5 presents a qualitative comparison of DeceptionX on a representative deceptive video clip, where two leading MLLMs both misclassify the sample as “Truthful”. Gemini focuses on “frequent

hand gestures” and “animated speech with varying tone”, interpreting them as natural storytelling. Meanwhile, Qwen emphasizes “expressive gestures”, “open palms”, “consistent eye contact”, and “fluent speech”, concluding that the subject exhibits a relaxed and truthful demeanor. These general-purpose MLLMs tend to rely on salient but superficial cues, failing to capture subtle deceptive signals. In contrast, DeceptionX extracts fine-grained multimodal evidence and links these observations to cognitive load, discomfort, and narrative distancing to construct a coherent chain of thought. This reasoning process directly mirrors the analytical patterns of human experts, intuitively demonstrating the superiority of DeceptionX in deception detection.

## 6 Conclusion

In this paper, we propose DeceptionX, a framework that reframes deception detection from a traditional binary classification task into an interpretable reasoning process. To support this framework, we construct a high-quality dataset, DeceptChain, through human-AI collaboration. In addition, we design a progressive training strategy and a redundancy elimination mechanism to enhance the model’s perception and reasoning capabilities. Experimental results show that DeceptionX outperforms existing MLLMs and specialized methods across multiple benchmarks, achieving significant improvements in both accuracy and reasoning quality. Ablation studies further validate the effectiveness of each component.

## Acknowledgments

To Robert, for the bagels and explaining CMYK and color spaces.

## References

- [1] Mohamed Abouelenien, Mihai Burzo, Verónica Pérez-Rosas, Rada Mihalcea, Haitian Sun, and Bohan Zhao. 2018. Gender differences in multimodal contact-free deception detection. *IEEE MultiMedia* 26, 3 (2018), 19–30.
- [2] Josh Achiam, Steven Adler, Sandhini Agarwal, Lama Ahmad, Ilge Akkaya, Florencia Leoni Aleman, Diogo Almeida, Janko Altmenschmidt, Sam Altman, Shyamal Anadkat, et al. 2023. Gpt-4 technical report. *arXiv preprint arXiv:2303.08774* (2023).
- [3] Chongyang Bai, Maksim Bolonkin, Judee Burgoon, Chao Chen, Norah Dunbar, Bharat Singh, VS Subrahmanian, and Zhe Wu. 2019. Automatic long-term deception detection in group interaction videos. In *2019 IEEE International Conference on Multimedia and Expo (ICME)*. IEEE, 1600–1605.
- [4] Chongyang Bai, Maksim Bolonkin, Viney Regunath, and VS Subrahmanian. 2022. POLLY: A multimodal cross-cultural context-sensitive framework to predict political lying from videos. In *Proceedings of the 2022 International Conference on Multimodal Interaction*. 520–530.
- [5] Jinze Bai, Shuai Bai, Yunfei Chu, Zeyu Cui, Kai Dang, Xiaodong Deng, Yang Fan, Wenbin Ge, Yu Han, Fei Huang, et al. 2023. Qwen technical report. *arXiv preprint arXiv:2309.16609* (2023).
- [6] Leo Breiman. 2001. Random forests. *Machine learning* 45, 1 (2001), 5–32.
- [7] Zesen Cheng, Sicong Leng, Hang Zhang, Yifei Xin, Xin Li, Guanzheng Chen, Yongxin Zhu, Wenqi Zhang, Ziyang Luo, Deli Zhao, et al. 2024. Videollama 2: Advancing spatial-temporal modeling and audio understanding in video-llms. *arXiv preprint arXiv:2406.07476* (2024).
- [8] Yunfei Chu, Jin Xu, Qian Yang, Haojie Wei, Xipin Wei, Zhifang Guo, Yichong Leng, Yuanjun Lv, Jinzheng He, Junyang Lin, et al. 2024. Qwen2-audio technical report. *arXiv preprint arXiv:2407.10759* (2024).
- [9] Yunfei Chu, Jin Xu, Xiaohuan Zhou, Qian Yang, Shiliang Zhang, Zhijie Yan, Chang Zhou, and Jingren Zhou. 2023. Qwen-audio: Advancing universal audio understanding via unified large-scale audio-language models. *arXiv preprint arXiv:2311.07919* (2023).
- [10] Alex Sebastião Constâncio, Denise Fukumi Tsunoda, Helena de Fátima Nunes Silva, Jocelaine Martins da Silveira, and Deborah Ribeiro Carvalho. 2023. Deception detection with machine learning: A systematic review and statistical analysis. *Plos one* 18, 2 (2023), e0281323.
- [11] Barry De Ville. 2013. Decision trees. *Wiley Interdisciplinary Reviews: Computational Statistics* 5, 6 (2013), 448–455.
- [12] Arianna D’Ulizia, Alessia D’Andrea, Patrizia Grifoni, and Fernando Ferri. 2024. Analysis, evaluation, and future directions on multimodal deception detection. *Technologies* 12, 5 (2024), 71.
- [13] Klaus Greff, Rupesh K Srivastava, Jan Koutnik, Bas R Steunebrink, and Jürgen Schmidhuber. 2016. LSTM: A search space odyssey. *IEEE transactions on neural networks and learning systems* 28, 10 (2016), 2222–2232.
- [14] Xiaobao Guo, Nithish Muthuchamy Selvaraj, Zitong Yu, Adams Wai-Kin Kong, Bingquan Shen, and Alex Kot. 2023. Audio-visual deception detection: Dolo-dataset and parameter-efficient crossmodal learning. In *Proceedings of the IEEE/CVF International Conference on Computer Vision*. 22135–22145.
- [15] Viresh Gupta, Mohit Agarwal, Manik Arora, Tanmoy Chakraborty, Richa Singh, and Mayank Vatsa. 2019. Bag-of-lies: A multimodal dataset for deception detection. In *Proceedings of the IEEE/CVF conference on computer vision and pattern recognition workshops*. 0–0.
- [16] Marti A. Hearst, Susan T Dumais, Edgar Osuna, John Platt, and Bernhard Scholkopf. 1998. Support vector machines. *IEEE Intelligent Systems and their applications* 13, 4 (1998), 18–28.
- [17] Binyuan Hui, Jian Yang, Zeyu Cui, Jiayi Yang, Dayiheng Liu, Lei Zhang, Tianyu Liu, Jiajun Zhang, Bowen Yu, Keming Lu, et al. 2024. Qwen2. 5-coder technical report. *arXiv preprint arXiv:2409.12186* (2024).
- [18] Jian Kang, Wen Qu, Shaoxing Cui, and Xiaoyi Feng. 2024. Deception detection algorithm based on global and local feature fusion with multi-head attention. In *2024 3rd International Conference on Image Processing and Media Computing (ICIPMC)*. IEEE, 162–168.
- [19] Mohan Karnati, Ayan Seal, Anis Yazidi, and Ondrej Krejcar. 2021. LieNet: a deep convolution neural network framework for detecting deception. *IEEE transactions on cognitive and developmental systems* 14, 3 (2021), 971–984.
- [20] Salman Khan, Muzammal Naseer, Munawar Hayat, Syed Waqas Zamir, Fahad Shahbaz Khan, and Mubarak Shah. 2022. Transformers in vision: A survey. *ACM computing surveys (CSUR)* 54, 10s (2022), 1–41.
- [21] Junnan Li, Dongxu Li, Silvio Savarese, and Steven Hoi. 2023. Blip-2: Bootstrapping language-image pre-training with frozen image encoders and large language models. In *International conference on machine learning*. PMLR, 19730–19742.
- [22] Zewen Li, Fan Liu, Wenjie Yang, Shouheng Peng, and Jun Zhou. 2021. A survey of convolutional neural networks: analysis, applications, and prospects. *IEEE transactions on neural networks and learning systems* 33, 12 (2021), 6999–7019.
- [23] Zheng Lian, Haoyu Chen, Lan Chen, Haiyang Sun, Licai Sun, Yong Ren, Zebang Cheng, Bin Liu, Rui Liu, Xiaojiang Peng, et al. 2025. Affectgpt: A new dataset, model, and benchmark for emotion understanding with multimodal large language models. *arXiv preprint arXiv:2501.16566* (2025).
- [24] Chin-Yew Lin. 2004. Rouge: A package for automatic evaluation of summaries. In *Text summarization branches out*. 74–81.
- [25] Haotian Liu, Chunyuan Li, Qingyang Wu, and Yong Jae Lee. 2023. Visual instruction tuning. *Advances in neural information processing systems* 36 (2023), 34892–34916.
- [26] E Paige Lloyd, Jason C Deska, Kurt Hugenberg, Allen R McConnell, Brandon T Humphrey, and Jonathan W Kunstman. 2019. Miami University deception detection database. *Behavior research methods* 51, 1 (2019), 429–439.
- [27] Jaume Masip. 2017. Deception detection: State of the art and future prospects. *Psicothema* 29, 2 (2017), 149–159.
- [28] Merylin Monaro, Stéphanie Maldera, Cristina Scarpazza, Giuseppe Sartori, and Nicolò Navarin. 2022. Detecting deception through facial expressions in a dataset of videotaped interviews: A comparison between human judges and machine learning models. *Computers in Human Behavior* 127 (2022), 107063.
- [29] Borum Nam, Joo Young Kim, Beomjun Bark, Yeongmyeong Kim, Jiyeon Kim, Soon Won So, Hyung Youn Choi, and In Young Kim. 2023. FacialCueNet: unmasking deception-an interpretable model for criminal interrogation using facial expressions: IY Kim et al. *Applied Intelligence* 53, 22 (2023), 27413–27427.
- [30] Kishore Papineni, Salim Roukos, Todd Ward, and Wei-Jing Zhu. 2002. Bleu: a method for automatic evaluation of machine translation. In *Proceedings of the 40th annual meeting of the Association for Computational Linguistics*. 311–318.
- [31] Verónica Pérez-Rosas, Mohamed Abouelenien, Rada Mihalcea, and Mihai Burzo. 2015. Deception detection using real-life trial data. In *Proceedings of the 2015 ACM on international conference on multimodal interaction*. 59–66.
- [32] Zhihong Shao, Peiyi Wang, Qihao Zhu, Runxin Xu, Junxiao Song, Xiao Bi, Haowei Zhang, Mingchuan Zhang, YK Li, Yang Wu, et al. 2024. Deepseekmath: Pushing the limits of mathematical reasoning in open language models. *arXiv preprint arXiv:2402.03300* (2024).
- [33] Felix Soldner, Verónica Pérez-Rosas, and Rada Mihalcea. 2019. Box of lies: Multimodal deception detection in dialogues. In *Proceedings of the 2019 Conference of the North American Chapter of the Association for Computational Linguistics: Human Language Technologies, Volume 1 (Long and Short Papers)*. 1768–1777.
- [34] Yixuan Su, Tian Lan, Huayang Li, Jialu Xu, Yan Wang, and Deng Cai. 2023. Pandagpt: One model to instruction-follow them all. In *Proceedings of the 1st Workshop on Taming Large Language Models: Controllability in the era of Interactive Assistants!* 11–23.
- [35] Pengjie Tang, Jiayu Zhang, Hanli Wang, Yunlan Tan, and Yun Yi. 2025. SRVCLA: Sparse regularization of visual context and latent attention based model for

- video description. *Neurocomputing* 630 (2025), 129639. doi:10.1016/j.neucom.2025.129639
- [36] Gemini Team, Rohan Anil, Sebastian Borgeaud, Jean-Baptiste Alayrac, Jiahui Yu, Radu Soricut, Johan Schalkwyk, Andrew M Dai, Anja Hauth, Katie Millican, et al. 2023. Gemini: a family of highly capable multimodal models. *arXiv preprint arXiv:2312.11805* (2023).
- [37] Peng Wang, Shuai Bai, Sinan Tan, Shijie Wang, Zhihao Fan, Jinze Bai, Keqin Chen, Xuejing Liu, Jialin Wang, Wenbin Ge, et al. 2024. Qwen2-vl: Enhancing vision-language model's perception of the world at any resolution. *arXiv preprint arXiv:2409.12191* (2024).
- [38] Taorui Wang, Xun Lin, Yong Xu, Qilang Ye, Dan Guo, Sergio Escalera, Ghada Khoriba, and Zitong Yu. 2026. Micro-gesture recognition: A comprehensive survey of datasets, methods, and challenges. *Machine Intelligence Research* 23, 2 (2026), 308–330.
- [39] Zhe Wu, Bharat Singh, Larry Davis, and V Subrahmanian. 2018. Deception detection in videos. In *Proceedings of the AAAI conference on artificial intelligence*, Vol. 32.
- [40] Jin Xu, Zhifang Guo, Jinzheng He, Hangrui Hu, Ting He, Shuai Bai, Keqin Chen, Jialin Wang, Yang Fan, Kai Dang, Bin Zhang, Xiong Wang, Yunfei Chu, and Junyang Lin. 2025. Qwen2.5-Omni Technical Report. arXiv:2503.20215 [cs.CL] <https://arxiv.org/abs/2503.20215>
- [41] An Yang, Anfeng Li, Baosong Yang, Beichen Zhang, Binyuan Hui, Bo Zheng, Bowen Yu, Chang Gao, Chengen Huang, Chenxu Lv, et al. 2025. Qwen3 technical report. *arXiv preprint arXiv:2505.09388* (2025).
- [42] Jiayu Zhang, Xun Lin, Jiajian Huang, Shuo Ye, Xiaobao Guo, Dongliang Zhu, Ruimin Hu, Dan Guo, Yanyan Liang, Zitong Yu, et al. 2026. Multimodal deception detection: A survey. *Machine Intelligence Research* 23, 2 (2026), 284–307.
- [43] Jiayu Zhang, Pengjie Tang, Yunlan Tan, and Hanli Wang. 2025. MGTR-MISS: More Ground Truth Retrieving based Multimodal Interaction and Semantic Supervision for video description. *Neural Networks* 192 (2025), 107817. doi:10.1016/j.neunet.2025.107817
- [44] Jiayu Zhang, Shuo Ye, Qilang Ye, Xun Lin, Zihan Song, and Zitong Yu. 2025. AV-Master: Dual-Path Comprehensive Perception Makes Better Audio-Visual Question Answering. *arXiv preprint arXiv:2510.18346* (2025).
- [45] Jiayu Zhang, Shuo Ye, Qilang Ye, Zihan Song, Jiajian Huang, and Zitong Yu. 2026. Retrieving to Recover: Towards Incomplete Audio-Visual Question Answering via Semantic-consistent Purification. arXiv:2604.10695 [cs.CV] <https://arxiv.org/abs/2604.10695>